Emerging specific selectivity towards mercury(II) cations in water through supramolecular assembly at interfaces

Elizaveta V Ermakova, Alexander V. Shokurov, Carlo Menon, Julien Michalak, Alla G. Bessmertnykh-Lemeune, Aslan Yu. Tsivadze, Vladimir V Arslanov

Emerging specific selectivity towards mercury(II) cations in water through supramolecular assembly at interfaces

Elizaveta V. Ermakova[a], Alexander V. Shokurov[b], Carlo Menon[b], Julien Michalak[c], Alla Bessmertnykh-Lemeune[c,d,*], Aslan Yu. Tsivadze[a,e], Vladimir V. Arslanov[a,*]

[a] *Frumkin Institute of Physical Chemistry and Electrochemistry, Russian Academy of Sciences, Leninsky Pr. 31, Moscow 119071, Russia*

[b] *Biomedical and Mobile Health Technology Lab, Department of Health Sciences and Technology, ETH Zürich, Lengghalde 5, Zürich 8008, Switzerland*

[c] *Institut de Chimie Moléculaire de l'Université de Bourgogne (ICMUB), UMR CNRS 6302, 9 avenue A. Savary, 21078 Dijon Cedex, France*

[d] *Laboratoire de Chimie, UMR 5182, CNRS, ENS de Lyon, 46 allée d'Italie, 69364, Lyon, Cedex, France*

[e] *N.S. Kurnakov Institute of General and Inorganic Chemistry of Russian Academy of Sciences, Leninsky pr. 31, Moscow 119071, Russia*

*E-mail: arslanov@phyche.ac.ru (Vladimir V. Arslanov), alla.lemeune@ens-lyon.fr (Alla Bessmertnykh-Lemeune)

KEYWORDS: aminoanthraquinone, chemosensor, mercury(II), copper(II), Langmuir-Blodgett film, selective detection

Abstract

This work deals with the development of ultra-thin film nanosensors for selective and sensitive detection of toxic Hg^{2+} cations in aqueous media. 1,8-Bis[(2-aminoethyl)amino]anthraquinone **D0** was functionalized by alkoxy groups of different length to prepare ligands **D3** and **D12** with linear arrangement of two polyamine receptors and two lipophilic alkyl chains. Chemosensor **D0** only binds copper(II) and mercury(II) cations in water/methanol (1:1 v/v) solutions with no interference by other metal cations. The introduction of alkoxy groups to the anthraquinone

scaffold, which are required to form Langmuir monolayers and ultra-thin films on solid supports, does not change the sensing properties of the anthraquinone **D0**. In contrast to systems without specific molecular order (i.e. solutions and drop-cast films**)**, Langmuir monolayers and ultra-thin Langmuir-Blodgett films of alkoxy-substituted ligands selectively bind only mercury(II) cations, even in the presence of copper(II) ions and 10 other interfering cations. Selective binding of mercury(II) cations was confirmed by the UV–vis absorption and X-ray fluorescence spectroscopies. Thus, ultra-thin films, in which chemosensor molecules are assembled in highly ordered supramolecular systems, display a higher selectivity as compared to that of disordered molecular systems. Ultra-thin sensory film allows for the selective detection of Hg^{2+} ions in water when their concentration is exceeded 0.01 μM, which corresponds to the action level for Hg^{2+} ions in drinking water recommended by the U.S. Environmental Protection Agency. Chemosensor **D12** is also suitable for the fabrication of electrochemical sensors for mercury(II) cations that show similar sensitivity.

1. Introduction

Nanotechnology is one of the key tools of modern sensory science, since it allows for both device miniaturization and use of specific physicochemical properties of compounds induced by structural ordering in low-dimensional systems. Nevertheless, little attention is currently paid to unusual properties of such low-dimensional systems, which in fact are their most attractive side [1-4].

This fully applies to the development of miniature and effective thin-film organic sensors as well as bilayer vesicular ones for determination of cations of toxic and biologically significant metals, which is one of the most important tasks of modern nanosensorics [5-9]. The advantages of such nanoscale sensors are their compactness, high performance, and availability of receptors for analytes. In recent years, research has been devoted to improvement of fabrication methods of ultra-thin sensitive layers, development of the new sensor materials, as well as searching for

new principles of sensor functioning that provide a high level of measured analytical characteristics [10-12]. To a large extent, this applies to such analytes as toxic metal cations [13].

One of the most promising approaches to such sensors are optical sensors [14, 15]. Optical chemosensors are modular molecules, each fragment of which performs one of the necessary functions, e.g. analyte binding, signal generation, etc. [16-23]. At the same time, the complication of the molecular structure of ligands, which is necessary in the design of selective molecular sensors, can obstruct processes of self-assembly of molecules and the formation of organized molecular layers at the interfaces, often required for efficient sensorics. We recently encountered this problem while investigating the sensing properties of ultra-thin Langmuir-Blodgett (LB) films obtained from amphiphilic modular anthraquinones bearing branched receptor groups [20]. Due to the low degree of the monolayer organization, from which multilayer LB films were assembled, they were subject to partial washing off the substrate upon exposure to aqueous solutions of analytes. We solved this problem by increasing the length of the alkoxy substituents at aromatic rings [20].

Since toxic ions are present in the environment (including biological objects), industrial and domestic wastewaters in form of aqueous solutions, sensitive layers of practically viable sensors should be both stable and be able to interact with the analyte cations in water. The latter requirement is often the focus of studies in optical sensors [24], as mostly chemosensors solutions are studied. At the same time cutting-edge developments in Hg^{2+} cations in water mostly deal with interfacial nanoscale systems [25-27], which offers higher practicality, reusability, and sometimes opens way to unusual and useful properties.

Here we report interesting examples of two-dimensional (2D) sensory systems (LB films) for monitoring toxic metal ions in water that exhibit higher selectivity compared to molecular precursors that can be used only in water/methanol solvent mixtures. In this regard, we investigate the fabrication of liquid and thin-film solid-state sensors from 1,8-bis[(2-aminoethyl)amino]anthraquinone (**D0**) [20, 28] and its amphiphilic derivatives **D3** and **D12,**

which are structurally adapted to Langmuir technology (Fig. 1). The signal unit (reporter) of these compounds is the photoactive anthraquinone moiety absorbing light in the visible region [21, 29, 30]. Useful optical properties and ease of covalent modifications of this aromatic backbone are the basis for their wide use as active elements of colorimetric sensors for monitoring various analytes and, above all, anions [30, 31] and toxic metal cations [21, 29]. Compound **D0** was reported by us as a parent ligand of water soluble chromophores with structurally complex ionophore units [20].

It is worth noting that chelator **D0** is related to 1,8-bis{[2-(dimethylamino)ethyl]amino}anthraquinone (**D***) and less symmetric chemosensors **D*1** and **D*2** (Fig. 1) proposed by Kaurs' group as selective colorimetric sensors for Cu^{2+} ions in water/methanol (1:1 v/v) solution [32, 33]. However, environmentally important and very toxic mercury(II) cations were not investigated as interference ions by this group. Moreover, the sensory properties of water insoluble ligand **D0**, despite its availability, have not yet been reported.

In this work, we show that ligand **D0** binds copper(II) and mercury(II) cations in water/methanol solutions (1:1 v/v). Sensing properties of chelators **D3** and **D12** are similar to those of the parent anthraquinone **D0** but these compounds can be assembled in monolayers at the air–water interface. We show that being organized into monolayers (**D3** and **D12**) and multilayer Langmuir–Blodgett films (**D12**) they not only allow for analysis of aqueous samples without addition of organic co-solvents, but selectively recognize only mercury(II) cations in them.

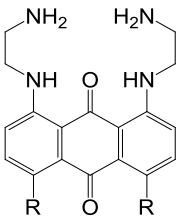

D0 R = H
D3 R = OC_3H_7
D12 R = $OC_{12}H_{25}$

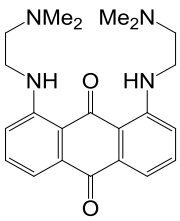

D*

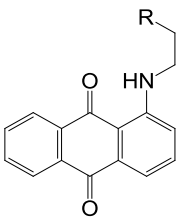

D*1 R = NH_2
D*2 R = NMe_2

Figure 1. Structure of the aminoanthraquinone ligands with simple receptor modules.

2. Experimental

2.1. General considerations

All chemicals were obtained from Fisher Scientific, Acros or Sigma-Aldrich. Chloroform (analytical grade) and methanol (99.8%) were purchased from Merck. All metal salts used were perchlorates of general $M(ClO_4)_n \cdot xH_2O$ formula. *Caution! Although no problems were experienced, perchlorate salts are potentially explosive when combined with organic ligands and should be manipulated with care and used only in very small quantities.* Analytical thin-layer chromatography (TLC) was carried out using Merck silica gel 60 F-254 plates (precoated sheets, 0.2 mm thick, with fluorescence indicator F254) and Merck DC Kieselgel 60 F-254 aluminum sheets. The spots were visualized directly or through illumination with UV lamp (λ = 254/365 nm). Column chromatography purification was carried out using silica gel 60 (40–63 μm) from Merck Co. Dioxane was distilled over sodium under argon. DMF (HPLC-grade), tetrachloromethane (HPLC-grade) and chloroform were obtained from Merck Co. and used without further purification. Acetone was dried over alumina cartridges using a solvent purification system PureSolv PS-MD-5 from Innovative Technology. 1,8-bis[(2-aminoethyl)amino]anthraquinone (**D0**) [28], 1,8-bis(dodecyloxy)anthraquinone [28], 1,8-dibromo-4,5-bis(dodecyloxy)anthraquinone (**2b**) [28] were prepared according procedures reported by us previously.

^{1}H and ^{13}C NMR spectra were acquired either on a Bruker Avance II 300 MHz, or Bruker Avance III 500 MHz spectrometers at room temperature. Chemical shifts are given in parts per million (ppm), referenced to residual non-deuterated solvent signals as internal standard. The coupling constants are expressed in units of frequency (Hz). FT-IR spectra were recorded with FT/IR-4200 Jasco spectrometer using a Jasco ATR PRO470-H accessory. Accurate mass measurements (HRMS) were carried out on a hybrid quadrupole-time-of-flight mass spectrometer Bruker microTOF-QII at the “Center de Spectrométrie de Masse”, University of

Lyon. Solutions in $CHCl_3$/methanol (1:1 v/v) were used for the analyses. The analyses were performed in positive mode using full scan MS with a mass range from 50 to 2000 Da at an acquisition rate of 1 Hz. The limit of detection (LOD) of copper(II) and mercury(II) ions was determined for ligands **D0**, **D3** and **D12** in water/methanol (1:1 v/v) solutions by UV–Vis spectrophotometry using the 3σ method [34].

*2.2. Synthesis of ligands **D3** and **D12**.*

1,8-Bis(propyloxy)-9,10-anthraquinone. A 250 mL two-necked flask equipped with a magnetic stirrer and a back-flow condenser was charged with 1,8-dihydroxy-9,10-anthraquinone (**1**) (1.0 g, 4.16 mmol), 1-bromopropane (1.13 mL, 1.53 g, 12.44 mmol) and cesium carbonate (6.10 g, 18.72 mmol). Subsequently, 7 mL of DMF and 20 mL of acetone was added and the mixture was stirred at reflux for 3 d. After cooling to room temperature, the reaction mixture was evaporated under reduced pressure. Then 400 mL of hot toluene was added and the suspension was filtered. The precipitate was washed with 25 mL of hot toluene and the filtrate was evaporated under reduced pressure. Recrystallization of the residue from acetone afforded the target compound as a yellow solid in 96% yield (1.29 g) after 24 h drying under reduced pressure. Mp 144–146 °C. IR (neat): ν_{max} (cm^{-1}) 2967m, 2837m, 2876m, 1667s, 1585s, 1576s, 1469m, 1453w, 1312s, 1279s, 1234w, 1218s, 1179m, 1061s, 1047w, 1017w, 953s, 899m, 888m, 788m, 739s, 657m, 823w, 603w. ^{1}H-NMR (300 MHz, $CDCl_3$): δ_H (ppm) 1.05 (t, 6H, J = 6.9, CH_3), 1.86 (m, 4H, CH_2), 4.02 (t, 4H, J = 6.9, CH_2O), 7.20 (dd, 2H, J = 7.5, J =1.0, ArH), 7.51 (t, 2H, J = 7.8, ArH), 7.73 (dd, 2H, J = 7.8, J =1.0, ArH). ^{13}C-NMR (75.5 MHz, $CDCl_3$): δ_H (ppm) 10.5 (2C, CH_3), 22.5 (2C, CH_2), 71.3 (2C, CH_2O), 118.8 (2C, ArCH), 119.6 (2C, ArCH), 124.8 (2C, quat Ar), 133.5 (2C, ArCH), 134.8 (2C, quat Ar), 158.9 (2C, quat Ar), 182.2 (1C, ArCO), 184.2 (1C, ArCO). HRMS (ESI): *m/z* calculated for $C_{20}H_{21}O_4$ ($M+H^+$) 325.1434, found 325.1436; $C_{20}H_{20}NaO_4$ ($M+Na^+$) 347.1254, found 347.1256.

1,8-Dibromo-4,5-bis(propyloxy)-9,10-anthraquinone (2a). A 50 mL two-necked flask equipped with a magnetic stirrer and a back-flow condenser was charged with 1,8-

bis(propyloxy)-9,10-anthraquinone (1.29 g, 3.98 mmol) and sodium acetate (2.14 g, 19.87 mmol), 10 mL of $CHCl_3$ and 10 mL of carbone tetrachloride. Then bromine was slowly added (8.32 g, 52.00 mmol) and the reaction mixture was heated for 15 h at 30 °C. After cooling to room temperature, 20 mL of $CHCl_3$ was added and the reaction mixture was washed with a saturated aqueous solution of sodium bisulfite (3 x 20 mL) and water (2 x 30 mL). The organic phase was dried with $MgSO_4$ and evaporated under reduced pressure. The crude product was recrystallized from heptane. The yellow solid **2a** was dried *in vacuo* for 24 h. Yield: 1.45 g (76%). Mp 202–203 °C. IR (neat): ν_{max} (cm^{-1}) 2967m, 2938m, 2875m, 1667s, 1585s, 1575bs, 1468m, 1453 m, 1437s, 1392m, 1312s, 1279m, 1233w, 1218s, 1178m, 1148w, 1113w, 1071s, 1018m, 953s, 899m, 888m, 840m, 830m, 793 m, 739s, 657m, 623w. ^{1}H-NMR (300 MHz, $CDCl_3$): δ_H (ppm) 1.01 (t, 6H, J = 6.9, CH_3), 1.81 (m, 4H, CH_2), 3.97 (t, 4H, J = 6.9, CH_2O), 6.94 (d, 2H, J = 9.0, ArH), 7.65 (d, 2H, J = 9.0, ArH). ^{13}C-NMR (75.5 MHz, $CDCl_3$): δ_H (ppm) 10.5 (2C, CH_3), 22.4 (2C, CH_2), 71.4 (2C, CH_2O), 110.1 (2C, quat Ar), 118.9 (2C, ArCH), 126.4 (2C, quat Ar), 134.8 (2C, ArCH), 139.3 (2C, quat Ar), 157.0 (2C, quat Ar), 180.7 (1C, ArCO), 184.2 (1C, ArCO). HRMS (ESI): *m/z* calculated for $C_{20}H_{19}Br_2O_4$ ($M+H^+$) 480.9645, found 480.9645; $C_{20}H_{20}NaO_4$ ($M+Na^+$) 347.1254, found 347.1256.

1,8-Bis[(2-aminoethyl)amino]-4,5-bis(propyloxy)-9,10-anthraquinone (**D3**) was prepared following modified reported procedure [28]. A 50 mL two-necked flask equipped with a magnetic stirrer and a back-flow condenser was charged with 1,8-dibromo-4,5-bis(propyloxy)-9,10-anthraquinone (**2a**) (0.50 g, 1.04 mmol), $Pd(dba)_2$ (60 mg, 0.10 mmol), BINAP (BINAP = 2,2′-bis(diphenylphosphino)-1,1′-binaphthyl; 129 mg, 0.21 mmol) and cesium carbonate (3.38 g, 10.37 mmol). The reaction vessel was evacuated and purged with N_2 three times. Then 30 mL of dioxane and 0.56 mL (10.37 mmol) of ethylenediamine was added by syringe and the reaction mixture was stirred at reflux for 2 d. After cooling to room temperature, the reaction mixture was filtered and evaporated under reduced pressure. The residue was purified by column chromatography on silica gel using gradient elution with CH_2Cl_2, CH_2Cl_2/MeOH (3:2 v/v) and

then CH_2Cl_2/MeOH/Et_3N (30:20:1 v/v/v) mixtures. Compound **D3** was isolated as a violet solid in 20% yield (92 mg). IR (neat): ν_{max} (cm^{-1}) 3283w, 3063w, 2961w, 2933w, 2874w, 1664m, 1619m, 1619m, 1596m, 1557m, 1539m, 1507s, 1461m, 1454m, 1388m, 1353m, 1264s, 1242m, 1194s, 1099m, 1061m, 1041m, 982m, 910s, 881s, 810m, 768w, 699w, 560w. ^{1}H-NMR (500 MHz, DMSO-*d6*): δ_H (ppm) 1.05 (t, 6H, *J* = 6.9, CH_3), 1.75 (m, 4H, CH_2), 2.87 (br t, 4H, *J* = 6.3, CH_2N), 3.34 (br q, 4H, *J* = 6.3, *CH_2*NHAr), 3.98 (t, 4H, *J* = 6.9, CH_2O), 7.14 (d, 2H, *J* = 9.4, ArH), 7.39 (d, 2H, *J* = 9.4, ArH), 9.30 (br t, 2H, *J* = 4.8, ArNH), NH_2 protons were not observed. Attempts to accumulate ^{13}C spectrum failed due to a low solubility of compound **D3**. HRMS (ESI): *m/z* calculated for $C_{24}H_{32}N_4O_4$ ($M+H^+$) 441.2496, found 441.2492.

1,8-Bis[(2-aminoethyl)amino]-4,5-bis(dodecyloxy)-9,10-anthraquinone (**D12**) was prepared following modified procedure reported in [28]. A 50 mL two-necked flask equipped with a magnetic stirrer and a back-flow condenser was charged with 1,8-dibromo-4,5-bis(dodecyloxy)-9,10-anthraquinone (**2b**) (1.00 g, 1.36 mmol), $Pd(dba)_2$ (78 mg, 0.14 mmol), BINAP (169 mg, 0.27 mmol) and cesium carbonate (4.44 g, 13.62 mmol). The reaction vessel was evacuated and purged with N_2 three times. Then 30 mL of dioxane and 0.91 mL (13.6 mmol) of ethylenediamine was added by syringe and the reaction mixture was stirred at reflux for 2 d. After cooling to room temperature, the reaction mixture was filtered and evaporated under reduced pressure. The residue was purified by column chromatography on silica gel using gradient elution with CH_2Cl_2, CH_2Cl_2/MeOH (3:2 v/v) and CH_2Cl_2/MeOH/Et_3N (60:40:1 v/v/v) mixtures. Compound **D12** was isolated as a violet solid in 23% yield (217 mg). The spectral data were in accordance with those reported by us previously [28]. IR (neat): ν_{max} (cm^{-1}) 3296m, 2922m, 2852m, 1668, 1620m, 1588m, 1565w, 1508s, 1461m, 1376w, 1358w, 1265s, 1193s, 1113w, 1048m, 909s, 881s, 815m, 722w, 700w. ^{1}H-NMR (300 MHz, $CDCl_3$): δ_H (ppm) 0.85 (t, 6H, *J* = 6.9, CH_3), 1.21 (br s, 32H), 1.43 (m, 4H, CH_2), 1.78 (m, 4H, CH_2), 3.01 (br t, 4H, *J* = 6.3, CH_2N), 3.35 (br q, 4H, *J* = 6.3, *CH_2*NHAr), 3.97 (t, 4H, *J* = 6.9, CH_2O), 6.89 (d, 2H, *J* =

9.4, ArH), 7.15 (d, 2H, *J* = 9.4, ArH), 9.30 (br t, 2H, *J* = 4.8, ArNH), NH_2 protons were not observed. Attempts to accumulate ^{13}C spectrum failed due to a low solubility of compound **D12**.

2.3. Visual detection of metal ions

The chemosensing properties of **D0**, **D3,** and **D12** in the presence of metal ions were evaluated visually by adding gradually up to 10 equiv. of a 0.05 – 0.1 M aqueous solution of metal perchlorate to **D0**, **D3** and **D12** (*c* = 0.022 – 0.045 mM) dissolved in a binary water/methanol solvent mixture (1:1 v/v).

2.4. UV–vis absorption measurements of solutions and LB films

The UV–vis absorbance spectra of solutions and LB films were recorded on a SHIMADZU-2450 spectrometer (Japan) in the 200–900 nm wavelength range. All UV–vis experiments with solutions were carried out in water/methanol (1:1 v/v) binary mixtures. The perchlorate salts were dissolved in pure water. LB films were transferred onto quartz substrate from air/water surface. Their UV spectra were recorded after exposition to analyte solutions, followed by washing with ultrapure water, and drying in air.

2.5. Preparation of Monolayers and LB films

A 1000-2 KSV Minitrough (*l* × *w* = 36.4 × 7.5 cm) model (KSV Instrument Ltd., Helsinki, Finland) equipped with a platinum Wilhelmy plate was used for preparation of Langmuir monolayers. The trough was made of PTFE and the barriers were made of polyacetal. Monolayers were formed by spreading a freshly prepared 0.1 mM chloroform solution of ligand onto the water surface. The solution volume deposited onto air–water interface was usually 75 μL. The spreading solution was deposited by means of a Gilson "Distriman" micropipette in 2.5 μL portions. Delivered drops were uniformly distributed over the available surface of water or aqueous solutions of perchlorate salts (0.001 – 1 mM). Deionized water (18.2 MΩ cm, pH ~5.5) produced by a Vodoley cartridge purificator (SPE Himelektronika, Russia) was used as a subphase.

After the sample has been spread, the solvent was allowed to evaporate for 15 min. All measurements were carried out at room temperature (20 ± 1 °C). The monolayer was compressed at a rate of 10 mm min^{-1}. Each compression isotherm was recorded at least three times to ensure the reproducibility of the results. The sensitivity of the Wilhelmy plate method for surface pressure–area (π–A) isotherms was ±0.01 mN m^{-1}.

LB-films were deposited onto quartz plates, cover glass or silicon supports. Transfer of monolayers was performed at a constant surface pressure of 5 or 20 mN m^{-1} by vertically immersing and withdrawing the solid substrate at a speed of 5 mm min^{-1} – upwards and 10 mm min^{-1} – downwards. Cast films were prepared by dropping the 0.1 mM chloroform solutions of the compound onto the surface of quartz substrate.

2.6. UV–vis reflection-absorption spectroscopy

UV–vis reflectance-absorbance spectra of Langmuir monolayers at the air–water interface was recorded in the 200–750 nm wavelength range using an AvaSpec–2048 FT–SPU (Avantes) fiber-optic spectrophotometer equipped with a 75 W DH-2000 deuterium-halogen light source and a CCD array detector. The UV–vis reflectometric probe with a fiber-optic diameter of 400 μm, combined with a 6–fiber irradiating bundle, was placed perpendicular to the studied surface at a distance of 2–3 mm. The signal reflected from the surface of the subphase prior to the deposition of the monolayer was used as a baseline.

2.7. Ultra-high resolution scanning electron microscopy (SEM)

SEM imaging was performed using the Field Emission Scanning Electron Microscope Zeiss Supra 55 (FE-SEM, Carl Zeiss, Germany). Accelerating voltage was set at 2-15 kV with 4-6 mm working distance. Imaging was conducted using in-Lens secondary electron detector. For SEM studies, the LB films were obtained on the cut silicon wafers.

2.8. X-ray Studies

X-ray patterns were acquired using Empyrean (Panalytical) diffractometer equipped with 1-D position-sensitive X'Celerator detector. Ni-filtered Cu Kα-radiation was employed.

Calibration of angular scale in low-angle region was verified using fresh silver behenate powder (Sigma Aldrich) [35]. Standard Bragg-Brentano (reflection) geometry was employed, allowing acquisition of out-of-plane diffraction, i.e., only planes parallel to the substrate are contributing. For X-ray studies, the LB films were obtained on the cut silicon wafers.

Elemental analysis of LB film was performed using an X-ray Analytical Microscope (XGT 7200, Horiba, Japan), with a Rhodium (Rh) X-ray tube, beam size of 1.2 mm, tube voltage of 30 kV, and current of 0.15 mA under vacuum.

2.9. Electrochemical impedance spectroscopy

Electrochemical impedance spectroscopy measurements were performed with an IPC-compact electronic potentiostat coupled with IPC-FRA2 frequency response analyzer, controlled by the Intelligent Potentiostat Control software (IPC-Compact ver. 8.65 developed at IPCE RAS, Moscow, Russia). The three-electrode cell was equipped with the working electrode (20 × 20 mm TF1 glass plate coated with the modified gold layer), a standard Ag/AgCl reference electrode, and a platinum wire as an auxiliary electrode. A solution of $K_3[Fe(CN)_6]$ and $K_4[Fe(CN)_6]$ (1 mM each) prepared in 0.5 M KCl was used as a redox-active probe. The cell was washed with deionized water and ethanol.

3. Results and discussion

3.1. Design and synthesis of aminoanthraquinones

Hydroxy- and halogen-substituted anthraquinones are valuable starting compounds to design and prepare colorimetric sensors exhibiting a high absorptivity in the visible region. Recently, we demonstrated that the Buchwald-Hartwig reaction is well suited to synthesize anthraquinones bearing polyamine receptor groups directly attached to the chromogenic aromatic fragment [36]. Because of a wide scope of this reaction, fine structural tuning of both ionophore and chromophore units of these ligands is possible to adapt the molecular structure to a target analyte and experimental conditions. In the case of LB films formation, the amphiphilic molecules with a linear arrangement of a polyamine receptor and a lipophilic alkyl chain are

required. Due to symmetry of the anthraquinone molecule the number of each of these groups can be doubled to favor intermolecular interactions, which, as in the case of lipid molecules, stabilize Langmuir monolayers, bilayers and LB films. Such derivatives can be obtained in three steps starting from 1,8-dihydroxyanthraquinone (**1**) (Scheme 1) [28]. The alkylation of this compound with appropriate primary bromides followed by the bromination of the anthraquinone moiety afforded selectively and in good yield alkoxy-substituted bromides **2a,b** which can be introduced in the Pd-catalyzed amination reaction to prepared target compounds. In continuation of our previous work on the catalytic amination of non-substituted 1,8-dichloroanthraquinone [20], we investigated the scope of this reaction and showed that the target alkoxy-substituted aromatic compounds with different alkyl chains (from one to eighteen) can be obtained in 20–25% yields using a $Pd(dba)_2$/BINAP catalytic system and cesium carbonate as a base. All compounds were successfully purified by column chromatography using a gradient elution with polar eluents such as CH_2Cl_2/MeOH and then CH_2Cl_2/MeOH/Et_3N mixtures adapting the maximal amount of Et_3N to the polarity of the target product. Propyloxy- and dodecyloxy-substituted ligands **D3** and **D12** were selected for this study. These chelators are insoluble in water and exhibit a rather low solubility in all polar organic solvents such as chloroform, methanol, DMSO and THF but their 0.01–0.1 mM solutions in chloroform and DMSO which are required for spectroscopic investigations and the preparation of Langmuir monolayers can be successfully obtained. To demonstrate the role of alkyl substituents in the formation of stable Langmuir monolayers, the parent 1,8-bis[(2-aminoethyl)amino]anthraquinone (**D0**) was also prepared in 41% yield (Scheme 1) [36].

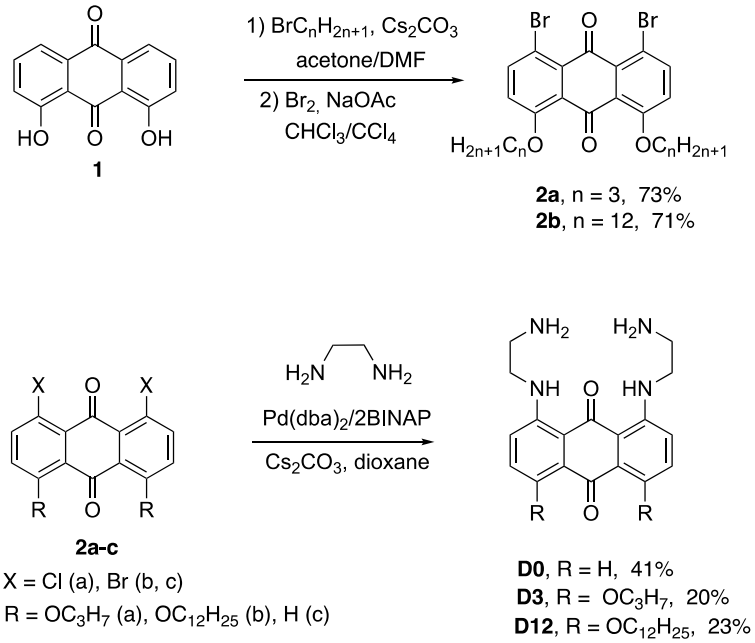

Scheme 1. Synthesis of anthraquinones **D0, D3** and **D12**.

3.2. Colorimetric sensing of metal ions by aminoanthraquinone ligands in solutions

Since anthraquinones **D0**, **D3**, and **D12** are insoluble in water, their optical responses toward 12 environmentally relevant metal ions were examined visually and by UV–vis spectroscopy in water/methanol (1:1 v/v) solutions. Sensing properties of three ligands were similar and color changes were observed only when the copper(II) and mercury(II) cations were introduced in their solutions (Fig. 2).

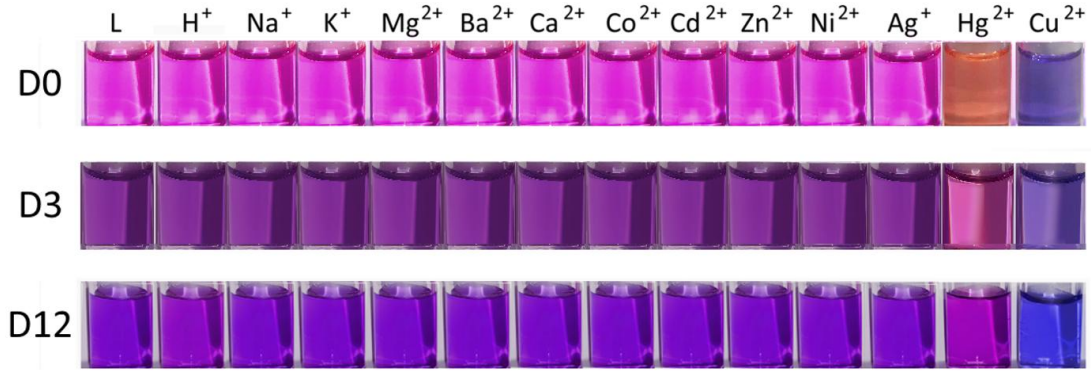

Fig. 2. Cation-induced color changes of **D0**, **D3,** and **D12** ligands in water/methanol (1:1 v/v) solutions (0.05 mM) upon addition of 10 equiv. of metal perchlorates or $HClO_4$ (pH>2).

As shown in Fig. 3a for ligand **D0**, sequential additions of 2 equiv. of copper(II) cations lead to a significant intensity decrease of the absorption band at 540 nm and the appearance of three bands in the long-wavelength region of the spectrum (at 645, 710, and 810 nm), that indicates the formation of a complex [32]. Further increase of the analyte concentration changes absorption bands only marginally.

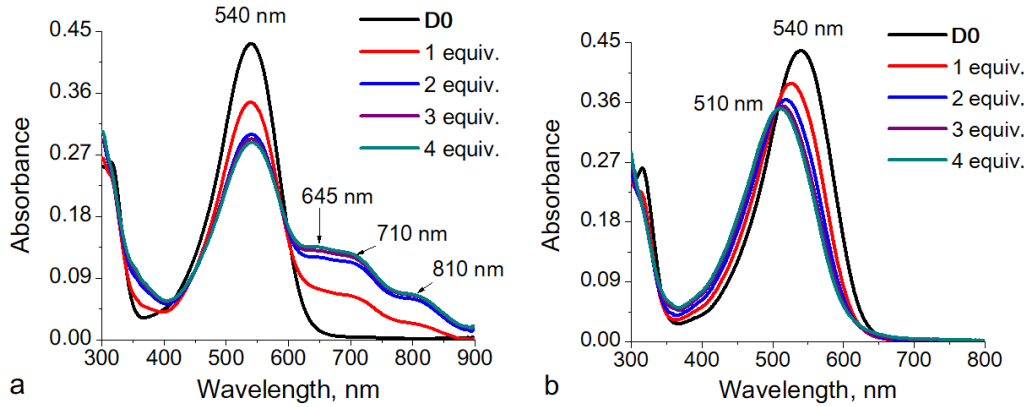

Fig. 3. Evolution of the UV–vis absorbance spectra of **D0** (0.045 mM) upon addition of $Cu(ClO_4)_2$ (0.01 M) (a) and $Hg(ClO_4)_2$ (0.002 M) (b) in water/methanol (1:1 v/v) solution, all spectra are corrected for dilution effects.

Kaur and Kumar [32] reported selective binding of Cu^{2+} ions by analogous diaminoanthraquinone **D*** (Fig. 1) in water/methanol (1:1 v/v) solution in the presence of Na^+, K^+, Mg^{2+}, Ca^{2+}, Sr^{2+}, Ba^{2+}, Ni^{2+}, Cd^{2+}, Co^{2+}, and Zn^{2+} cations. At the same time, environmentally important and very toxic cations such as Hg^{2+} ions have not been considered in their work.

We have found that the addition of 1–4 equiv. of mercury(II) cations to the water/methanol solution of ligand **D0** leads to a hypsochromic shift of the absorbance band by 30 nm (Fig. 3b), while the color of the solution changes from pink to peach (Fig. 2). It is worth noting that the spectral properties of mercury(II) complex with ligand **D0** significantly differ from that of copper(II) complex probably due to another binding mode of the metal ion to the chelator. A metal-induced hypsochromic shift was previously observed for the water soluble aminoanthraquinones in the presence of mercury(II), lead(II), and cadmium(II) cations [20, 28, 37]. The hypsochromic shift is also typical for all aromatic ligands bearing donor groups at

aromatic rings due to a change of their electronic structure after coordination of metal ions. The bathochromic shift of the absorption maximum after formation of Cu^{2+} complexes with aminoanthraquinones was previously explained by the ligand deprotonation in the coordination sphere of this metal ion [20, 28, 37].

Similar results were obtained for the alkoxy-substituted chemosensors **D3** and **D12** and both cations as shown in Fig. 2 and Fig S1, but the spectral changes were less pronounced probably due to the introduction of two electron donating substituents (alkoxy groups) in the aromatic moiety and/or partial aggregation of these amphiphilic ligands in solution.

The detection limits of Cu^{2+} and Hg^{2+} cations were determined by cascade dilution experiments of the initial solutions of the complexes [37], formed by mixing aqueous solutions of metal perchlorates and water/methanol (1:1 v/v) solutions of ligands **D0, D3,** and **D12** (Table S1) using the 3σ method [34]. According to the analytical data summarized in Table S1, which were obtained using UV–vis absorbance spectroscopy and visual control of the solutions, ligand **D0** provides sensing of copper(II) and mercury(II) cations with a rather high sensitivity, demonstrates detectable concentrations of 0.017 mM by naked eye for both cations as well as 9.32 μM for Cu^{2+} and 0.64 μM for Hg^{2+} by spectrophotometer (Fig. S2-S7). Similar sensory characteristics are obtained for other two ligands **D3** and **D12**.

No spectral changes were also observed in the presence of other (K^+, Na^+, Mg^{2+}, Ba^{2+}, Ca^{2+}, Zn^{2+}, Co^{2+}, Cd^{2+}, Ag^+, Ni^{2+}) interference metal cations (Fig. S8 - S10).

3.3. Monolayers of amphiphilic aminoanthraquinone ligands on the surface of aqueous solutions of metal salts. Complexation from subphase

The ability of anthraquinone derivatives to form stable Langmuir monolayers is dependent on the substituents on the anthraquinone moiety. Ligand **D0** in which the anthraquinone ring has only two hydrophilic ethylenediamine residues does not form the monolayers. Amphiphilic ligands **D3** and **D12**, in which the hydrocarbon chain length differs by

a factor of 4, both form stable monolayers at the air–water interface, as indicated by reproducibility of Langmuir monolayer compression isotherms obtained (Fig. 4 a, c).

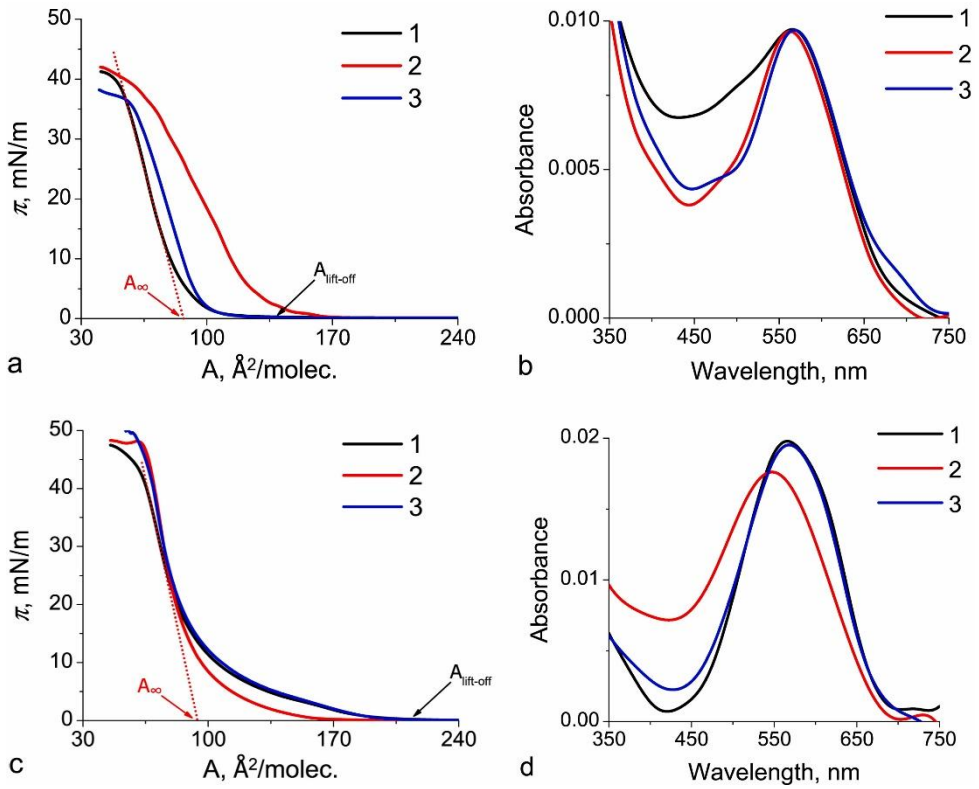

Fig. 4. Surface pressure vs area isotherms (a, c) and *in situ* UV–vis reflectance-absorbance spectra (b, d) for the monolayers of **D3** (a, b) and **D12** (c, d) on the surface of pure water (*1*) and on the 1 mM $Hg(ClO_4)_2$ (*2*) and $Cu(ClO_4)_2$ (*3*) aqueous solutions recorded at surface pressure 15 mN m^{-1}. Equilibration time before compression was 15 min (1) and 60 min (2–3), respectively.

Indeed, the position and the shape of the compression isotherms of two studied compounds are rather similar (Fig. 4a, c). The main difference lies in the area of the liquid-expanded state: this region for the long-chain surfactant **D12** is much larger than that of **D3**. The onset area of this state ($A_{lift\text{-}off}$) for the **D12** monolayer is about 70% larger, and the transition pressure to the condensed state is 2 times higher than the corresponding parameters of **D3** monolayer.

At the same time, the similarity of the extrapolated areas for linear sections of isotherms (A_∞), as well as comparable and high values of collapse surface pressures of two monolayers,

indicate an important role of the aminoanthraquinone fragment in the formation of monolayers, especially in the condensed state. This behavior of aromatic fragments strongly distinguishes anthraquinone derivatives from polycyclic hydrocarbons, porphyrins, phthalocyanines and analogous compounds used in development of optical chemosensor monolayers. Since A_∞ are close for both ligands and correspond to the area of the aromatic scaffold [38], it seems that anthraquinone molecules in the monolayers are almost parallel to the water surface regardless of the chain length.

The copper(II) cations introduced into the subphase do not significantly affect the compression isotherms of both ligands (Fig. 4 a, c). More surprisingly, the presence of copper(II) cations in the subphase does not change the UV–Vis reflectance-absorbance spectra of the monolayers (Fig. 4 b, d and S11-S12), in contrast to what was observed in water/methanol (1:1 v/v) solutions. No spectral changes are also observed for the monolayers of **D3** and **D12** in the presence of 10 other metal ions such as K^+, Na^+, Mg^{2+}, Ba^{2+}, Ca^{2+}, Zn^{2+}, Co^{2+}, Cd^{2+}, Ag^+, and Ni^{2+} in the subphase (Fig. S13).

On the other hand, both monolayers bind mercury(II) cations, as evidenced by the hypsochromic shifts of absorption bands in the *in situ* UV–vis reflectance-absorbance spectra after addition of Hg^{2+} ions (Fig.4 b, d and S11-S12). No less unexpected was the fact that a change in pH has practically no effect on the shape and position of the absorption bands both for the free **D12** monolayer and for its complex with mercury(II) cations (Fig. S14 a, c). According to the calibration curve, **D12** monolayer allows for detection of the Hg^{2+}ions at least up to 1 μM monitoring the absorbance at 570 nm, for instance. (Fig. S15).

Binding of mercury(II) cations leads to different changes in compression isotherms of the monolayers. The complexation affords a significant expansion of the **D3** monolayer, which is probably caused by long-range electrostatic repulsive forces between the charged molecules of the complexes, as it was observed in calixarene monolayers, for example [39]. In contrast,

monolayer formed by **D12** does not expand likely because these columbic interactions are screened by long hydrocarbon chains.

Thus, ligands **D3** and **D12** being organized in monolayers at the air–water interface display enhanced selectivity towards Hg^{2+} ions, since they lose their ability to bind Cu^{2+} ions.

This behavior may be due to the fact that the complexation of aminoanthraquinones with copper(II) cations in solution is accompanied by the deprotonation of the aromatic amino groups [20, 28, 37]. Such complexation processes are highly sensitive to the environmental polarity, which differs drastically between water/methanol solution and a monolayer on the water surface. The binding of copper(II) cations by the ligand is not observed even upon increase of the subphase pH up to 9, that could contribute to the deprotonation of amino groups in the Cu^{2+} complex (Fig. S14 b). We cannot also exclude that the highly uniform molecular orientation of chelator molecules in the monolayer leads to the formation of complexes with participation of neighboring chemosensor molecules which are spectrally silent. Probably mercury(II) ions match the spatial arrangement of chelator in the monolayer better than copper(II) ions because this ion displays various coordination numbers, which may facilitate its coordination by the structurally rather rigid monolayers.

Thus, being organized in planar supramolecular systems (Langmuir monolayers) chemosensors **D3** and **D12** exhibit a high sensitivity and exceptional selectivity in detection of mercury(II) cations in an aqueous medium. Such supramolecular systems also allow to perform the analysis without adding organic solvents such as methanol which are required when chemosensors **D3** and **D12** are used in liquid phase.

The very fact of elimination of competitive binding of a cation that previously interfered with detection of mercury(II) cations by the studied ligands is interesting not only from fundamental standpoint. Understanding and exploitation of this phenomenon can open new perspectives for highly efficient sensorics for Hg^{2+} in water, since copper(II) ions are usually present in media where levels of mercury(II) ions are analyzed. However, in order to actually

perform analysis in a practical manner, these sensitive monolayers need to be transferred onto solid substrates to form useable solid-state nanoscale sensors.

*3.4. Langmuir-Blodgett films of amphiphilic ligand **D12** as sensitive working element of planar optical sensors*

Since the monolayer transfer onto solid substrates by Langmuir-Blodgett method usually allows to retain the molecular organization, one could expect that selectivity to Hg^{2+} recognition will be also observed in these solid sensors prepared by this technique. Unfortunately, the transfer of the short-chain ligand **D3** onto a quartz substrate was inefficient. The transfer ratio of the second layer did not exceed 0.5 due to weak interactions of short hydrocarbon chains and most of the film was washed off during the third layer deposition. In contrast, multilayer Langmuir-Blodgett films of **D12** display high stability due to stronger interactions of alkyl chains as compared to those observed in the films of **D3** chemosensor. The film composed of 10 layers was not washed off from the slide after exposure to aqueous solutions with different pH values for 5 minutes as was demonstrated by the UV–vis spectroscopy (Fig. S16).

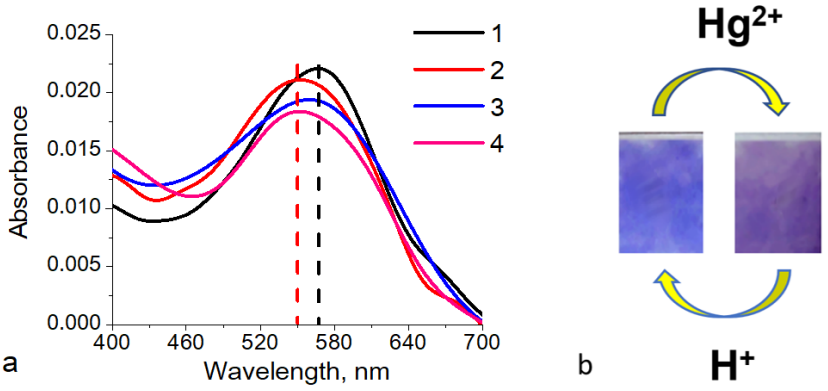

Fig. 5. (a) UV–vis absorbance spectra of LB film of **D12** (10 layers) deposited onto a quartz substrate from a surface of pure water at 20 mN m^{-1} (1) and sequentially immersed in 0.1 mM aqueous solution of $Hg(ClO_4)_2$ for 20 s (2), in HCl aqueous solution with pH 2 for 10 s (3) and in 0.1 mM aqueous solution of $Hg(ClO_4)_2$ for 20 s (4). Dashed lines show the wavelength of the absorbance maximum observed for free ligand (black line) and mercury complex (red line). (b) Cation-induced color changes in LB film of **D12** (20 layers) deposited onto a quartz substrate

from a surface of pure water at 20 mN m^{-1} and immersed in 1 mM aqueous solution of $Hg(ClO_4)_2$ for 10 min.

Immersion of this LB film in 0.1 mM aqueous solution of Hg^{2+} cations caused a hypsochromic shift of the absorbance band by 20 nm in less than 20 s. (Fig. 5a). When this film was treated by 0.1 M HCl solution for 10 s, a bathochromic shift of the absorbance maximum by 17 nm was observed. Apparently, the decomplexation of the mercury(II) under these conditions was accompanied by the protonation of ethylenediamine fragments. The sensor film thus regenerated retained both selectivity and a response time when it was reused in sensing of mercury(II) ions.

The LB film composed of 10 layers of **D12** immersed in a 0.1 mM aqueous solution of copper(II) cations for 300 s did not show any spectral response (Fig. S17). No spectral changes were also observed in the presence of other (K^+, Na^+, Mg^{2+}, Ba^{2+}, Ca^{2+}, Zn^{2+}, Co^{2+}, Cd^{2+}, Ag^+, Ni^{2+}) interference metal cations (Fig. S17).

The presence only of mercury(II) ions in the LB film of **D12** was also confirmed by X-ray fluorescence spectroscopy. The spectrum of a 20-layers LB film deposited onto a silicon surface immersed in aqueous solution of 11 metal cations, including copper (Fig. 6, black line) shows no mercury emission lines. Immersion in the same solution but with added Hg^{2+} ions leads to a spectrum with distinct Hg L emission lines (Fig. 6, red line).

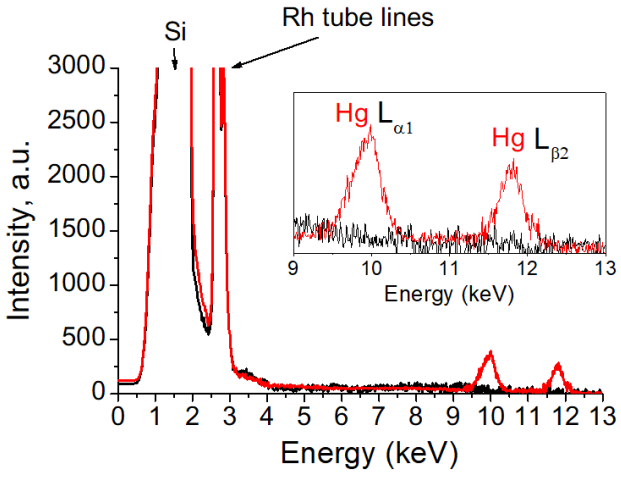

Fig. 6. X-ray fluorescence spectra of 20-layer LB film of **D12** transferred onto a cut silicon wafer at a surface pressure of 20 mNm^{-1} from the surface of deionized water. The spectra were recorded for the LB film that was immersed in aqueous solutions of metal perchlorates $M^{n+}(ClO_4)_n$, M = Cu^{2+}, K^+, Na^+, Mg^{2+}, Ba^{2+}, Ca^{2+}, Zn^{2+}, Co^{2+}, Cd^{2+}, Ag^+, Ni^{2+} (1 mM) (black line) and $M^{n+}(ClO_4)_n$ (1 mM) + $Hg(ClO_4)_2$ (0.1 mM) (red line).

To confirm that the supramolecular organization of the film is required for selective recognition of Hg^{2+} ions, drop-cast films of the **D12** ligand were prepared by spreading of a 0.1 mM chloroform solution of the chemosensor onto a pure quartz slide and subsequent drying of the slide for 60 min in air. These films bound both mercury(II) and copper(II) cations from aqueous solutions giving spectral responses analogous to those observed for methanol/water solutions of the chemosensor (Fig. S18).

Thus, comparing the selectivity of the chemosensor **D12** in water/methanol (1:1 v/v) solution, in cast, and in LB films, it can be concluded that the supramolecular organization of **D12** molecules is required to get the selective optical response on the mercury(II) ions. The absence of copper(II) cations complexation with **D12** in the LB film can be thus explained by the unfavorable arrangement of nitrogen donor groups in the film and/or by unfavorable change of their acidity in the organized molecular system. In any way, it is the high ordering in the LB films and supramolecular assembly of the chemosensor molecules that provides high selectivity towards aqueous Hg^{2+}.

LB films of **D12** demonstrate very high sensitivity for mercury(II) cations when employing spectral analysis, while only a small amount of the chemosensor substance is used to prepare the sensor film: e.g. 1 mg is enough to produce more than 300 ultra-thin film sensors on solid substrates. The film formed in such a way containing only 10 layers gives a distinct spectral response (20 nm shift of the absorbance band) in 0.01 μM mercury perchlorate aqueous solution after 80 s of immersion (Fig. S19). This value corresponds to the action level for Hg^{2+} ions in drinking water recommended by the U.S. Environmental Protection Agency (EPA) (2 ppb, 0.01

μM) [40]. It is also worth noting that sensitivity of thin-film sensor is higher than those of water soluble colorimetric chemosensors based on the amino-containing receptor group, which were studied by us previously [20, 28].

To get a reliable visual response of LB film upon metal ions recognition, the number of layers in the **D12** film should be increased up to 20. Such films show a rather intense color, which changes upon binding of mercury(II) cations (Fig. 5b).

*3.5. Electrochemical impedance spectroscopy detection of Hg^{2+} ions using the SAM/LBF-**D12** bilayer sensor*

High stability, selectivity, and sensitivity of LB films formed by anthraquinone **D12** on a quartz surface prompted us to investigate its deposition onto a thiol-modified gold surface to develop an electrochemical nanosensor which under specific experimental conditions can be more convenient for the analysis of real-life samples as compared to optical sensors.

To achieve a favorable orientation of chemosensor molecules, in which receptor groups are directed towards the analyte solution, a bilayer film was prepared on a gold electrode surface. First, a rarefied self-assembled monolayer (SAM) of octanethiol was formed on this surface, and then one monolayer of ligand **D12** was transferred onto it by the LB method in the top-down mode at 20 mN m^{-1} (one layer LB film, LBF-**D12**) [19]. The electrochemical behavior of the modified gold electrode was investigated by electrochemical impedance spectroscopy (EIS). The bilayer chip thus prepared was used as a working electrode in a standard three-electrode cell with the standard Fe^{3+}/Fe^{2+} redox couple solution (1 mM $K_3[Fe(CN)_6]$ + 1 mM $K_4[Fe(CN)_6]$ + 0.5 M KCl).

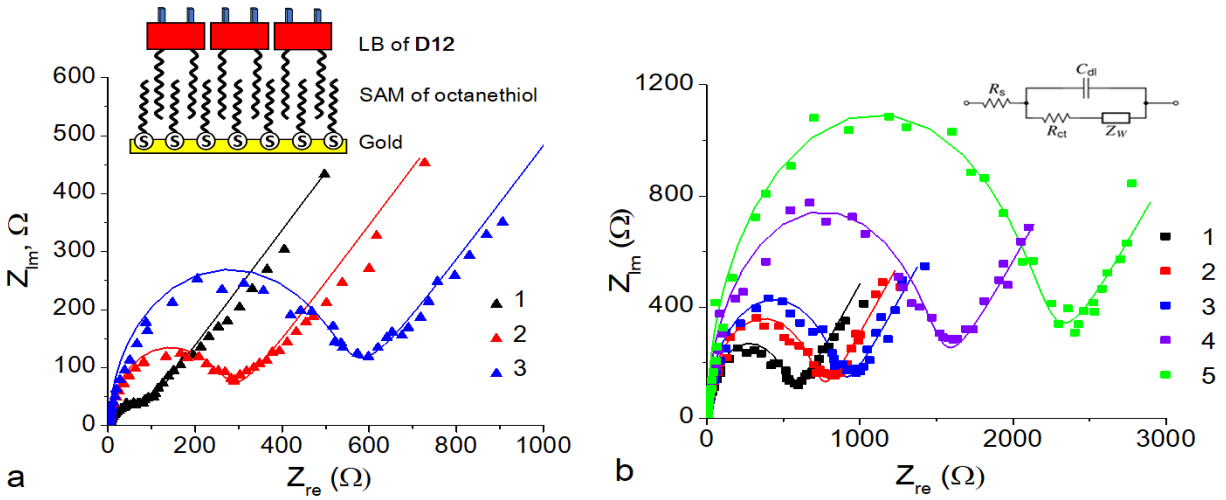

Fig. 7. Nyquist plots (hodographs) of (a): bare gold electrode (*1*); gold electrode coated with a SAM of octanethiol (*2*); SAM/LBF-**D12** bilayer (*3*); (b): SAM/LBF-**D12** bilayer before (*1*) and after exposure in an aqueous solution of $Hg(ClO_4)_2$ – (*2*) 0.01, (*3*) 0.10, (*4*) 1.00 and (*5*) 10.00 μM for 15 minutes. The insets show (a) schematic representation of SAM/LBF-**D12** bilayer and (b) the equivalent Randles circuit used for EIS data modeling.

Table 1. Electrochemical parameters obtained for bare and modified gold electrodes from theoretical modeling of the corresponding Nyquist plots, according to the equivalent Randles circuit presented on the inset of Fig. 7b

System	Hg^{2+} (μM)	R_s[a] (Ω)	C_{dl}[b] (μF/cm^2)	R_{ct}[c] (Ω/cm^2)	Z_W[d] (Ω/s$^{1/2}$)	θ[e]
Au	-	4.6	17.2	61.1	268.3	-
Au/SAM	-	3.9	9.5	253.9	281.2	-
Au/SAM/LBF-**D12**	-	4.1	8.1	517.9	294.7	0
Au SAM/LBF-**D12**	0.01	4.6	5.4	698.1	323.1	0.26
Au/SAM/LBF-**D12**	0.1	4.4	5.4	832.3	331.4	0.38
Au/SAM/LBF-**D12**	1	4.6	5.4	1448.1	421.6	0.64

Au/SAM/LBF-**D12**	10	5.0	5.0	2138.2	466.9	0.76

[a]R_s: electrolyte resistance. [b]C_{dl}: electrical double layer capacity. [c]R_{ct}: charge transfer resistance at the electrode/electrolyte interface. [d]Z_W: Warburg diffusion element. [e]θ: fractional coverage of the sensor surface by Hg^{2+} ions.

The electrochemical impedance spectra presented in the form of Nyquist plots, as well as the results of theoretical modeling using the classical Randles equivalent circuit, are provided in Fig. 7 and in Table 1, respectively. It can be seen that during the bilayer SAM/LBF-**D12** formation, as well as during the bilayer exposure to aqueous solutions of mercury(II) cations with increasing concentration, an increase in values of electrochemical characteristics (charge transfer resistance R_{ct} and Warburg diffusion element Z_W) is observed, reflecting the compaction of the sensitive layer. Fractional coverage of the sensor surface by Hg^{2+} ions (θ) was evaluated by comparing the charge transfer resistance of the bare Au/SAM/LBF-**D12** electrode (R_{ct}) to that of the system exposed to mercury(II) cations ($R_{ct'}$) by use of equation (1). The results of this estimation are presented in Table 1. [41]

$$\theta = 1 - R_{ct}/R_{ct'} \quad (1)$$

The surface coverage increases with the Hg^{2+} concentration and reaches rather high values indicating the accessibility of binding sites in the sensory layer for the analyte.

The electrochemical sensor based on SAM/LBF-**D12** bilayer allowing detection of mercury(II) ions at the 0.01 μM level (Fig. S20), which is comparable to the thin-film solid-state optical sensor based on the multilayer LB film of ligand **D12**. It worth noting that change of signal transduction mechanism from optical to electrochemical allows to decrease the thickness of working film from 10 sensory layers to only one thus increasing the sensitivity/amount of chemosensor ratio that is a major goal in preparation of advanced sensory systems.

*3.6. The morphology and structure of solid-state film sensors based on LB film of **D12***

The morphology and structure of LB films before and after complexation of mercury(II) cations was investigated by scanning electron microscopy and X-ray diffraction analysis. SEM images of LB film of **D12** transferred onto a silicon substrate at a surface pressure of 5 and 20 mN m^{-1} from the surface of deionized water show uniform coverage of the surface (Fig. 8). The higher the surface pressure of the film transfer, the more homogeneous and denser is the film (Fig. 8a,b). This can be explained by a higher degree of order in **D12** monolayers on the water surface with increasing the surface pressure. Upon coordination of mercury(II) cations by the film transferred at 20 mN m^{-1}, its morphology changes only slightly even when the exposure time was prolonged up to 1 hour. This observation agrees well with the behavior of **D12** Langmuir monolayers on water surface, as it was demonstrated that compression isotherms of **D12** monolayers before and after Hg^{2+} binding almost do not change (Fig. 4c), indicating absence of significant structural changes. A small change, however, can be noticed in the SEM images of the film on solid substrate: small aggregates evenly distributed over the entire film become more distinct, probably due to an increase of the electron density upon binding of mercury(II) cations (Fig. 8 c).

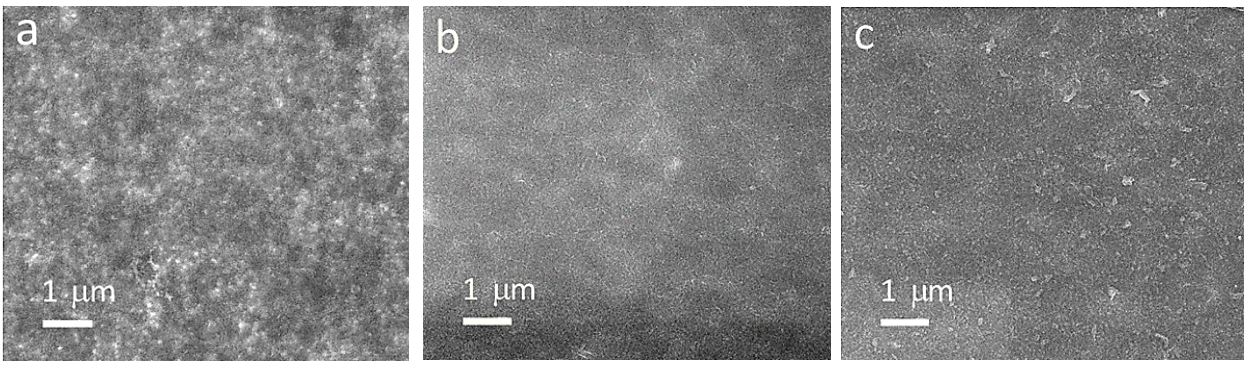

Fig. 8. SEM images of multilayer LB film of **D12**, transferred onto a cut silicon wafer at a surface pressure of 5 mN m^{-1} (a) and 20 mN m^{-1} (b, c) from the surface of deionized water, in total 20 layers. (c) LB film shown in frame *b*, but after exposure to 1 mM $Hg(ClO_4)_2$ aqueous solution.

X-ray diffraction of the 20-layer LB film, transferred at 20 mN m^{-1} onto silicon wafer, demonstrates a lamellar structure. Two distinct peaks observed in the diffractogram indicate the existence of two interplanar spacings in the film (Fig. 9, curve 1). After binding mercury(II) cations, the LB film retains this structural organization but interplanar spacing is decreased (Fig. 9, curve 2). This indicates that Hg^{2+} cation complexation leads to the formation of a more compact structure. This is also supported by the electrochemical impedance data and SEM images of the LB film.

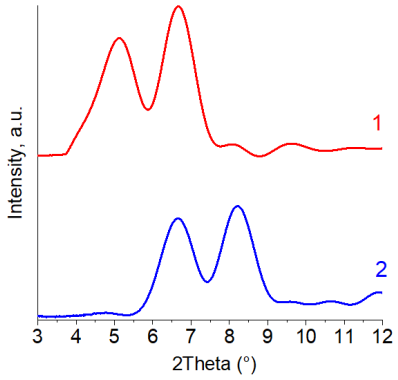

Fig. 9. X-ray diffraction patterns of multilayer LB film of **D12** transferred onto a cut silicon wafer at a surface pressure of 20 mNm^{-1} from the surface of pure water, in total 20 layers (*1*); LB film after exposure to 1 mM $Hg(ClO_4)_2$ aqueous solution (*2*).

4. Conclusions

Anthraquinones **D0**, **D3**, and **D12** with (2-aminoethyl)amine receptor units and various hydrophilic-lipophilic balance were prepared and investigated in sensing toxic metal ions in aqueous media. All these compounds are suitable for sensing of copper(II) and mercury(II) cations in water/methanol (1:1 v/v) solutions. Considering the 135 nm gap between the absorption maxima of mercury(II) and copper(II) complexes, simultaneous colorimetric monitoring of both cations can be envisaged. The presence of 10 (K^+, Na^+, Mg^{2+}, Ba^{2+}, Ca^{2+}, Zn^{2+}, Co^{2+}, Cd^{2+}, Ag^+, and Ni^{2+}) environmentally relevant metal ions does not affect the optical response of chemosensors to target copper(II) and/or mercury(II) cations.

We have shown that both amphiphilic derivatives – **D3** and **D12 –** formed stable Langmuir monolayers at the air–water interface, in which the aromatic fragment is oriented almost parallel to the water surface. This distinguishes anthraquinones from many other aromatic compounds (porphyrins, phthalocyanines, etc.) used in ultra-thin optical chemosensor research, which generally display a slipped stack-of-card orientation of the molecules in monolayers and exhibit strong π–π stacking. Due to this unusual orientation of the aromatic fragment, even the ligand with 3 carbon atom hydrocarbon chains (**D3**) forms stable non-aggregated monolayers on the water surface. After organization in Langmuir monolayers, chemosensors **D3** and **D12** lose their sensing ability towards copper(II) ions and display selective optical response to the presence of mercury(II) ions in water. This behavior effectively increases their selectivity towards mercury(II) cations.

LB films of various thicknesses were successfully prepared by deposition of **D12** monolayers onto quartz slides. These solid-state sensors also showed the increase of mercury(II) recognition selectivity and sensitivity as compared to their molecular precursor **D0**, which can be used only in water/methanol solution. The films exhibited exceptional selectivity for mercury(II) cations, as was demonstrated by UV–vis spectroscopy and X-ray fluorescence spectroscopy. The 10-layer LB film displays a spectral detection limit for Hg^{2+} in water of 0.01 μM, which corresponds to the action level for Hg^{2+} ions in drinking water recommended by the U.S. Environmental Protection Agency (EPA). Structural and morphological transformations in the sensitive LB layer upon binding of mercury(II) cations were investigated by X-ray diffraction and scanning electron microscopy.

The importance of supramolecular organization in LB films for sensor properties was demonstrated performing comparative studies of these films and the drop-cast film of chemosensor **D12.** The cast films with a random molecular orientation gave optical responses towards both copper(II) and mercury(II) cations in water, as was the case of the ligand solution.

The electrochemical impendence spectroscopy sensor was prepared by transfer of one monolayer of **D12** onto the surface of thiol-modified gold slides. This bilayer sensor displays similar sensitivity and allows for the selective detection of the Hg^{2+}ions up to 0.01 μM in aqueous solutions.

Thus, aminoanthraquinones with simple receptor groups were identified as promising compounds for preparation of optical and electrochemical sensors by using Langmuir techniques. The studied chemosensor shows an interesting effect, where selectivity towards recognition of Hg^{2+} emerges only in systems with supramolecular assembly within nanoscale Langmuir monolayers and even multilayer Langmuir-Blodgett films. This behavior demonstrates that not only the chemical structure of a molecular sensor *per se* is important in question of selectivity, but also the way the molecules are organized in the functional system used for sensor applications.

Acknowledgments

The work was supported by the Ministry of Science and Higher Education of Russia (grant agreement №075-15-2020-782). Structural measurements were performed using equipment of CKP FMI IPCE RAS. The authors acknowledge Dr. Alexander E. Baranchikov and Dr. Andrey A. Shiryaev for technical support and useful discussions.

Appendix A. Supplementary data

Supplementary data to this article can be found online at https://doi.org/.

REFERENCES

[1] Abdel-Karim R, Reda Y, Abdel-Fattah A. Nanostructured materials-based nanosensors. J Electrochem Soc. 2020;167(3):037554. https://doi.org/10.1149/1945-7111/ab67aa.

[2] Bogue R. Nanosensors: a review of recent research. Sens Rev. 2009;29(4):310-315. https://doi.org/10.1108/02602280910986539.

[3] Jianrong C, Yuqing M, Nongyue H, Xiaohua W, Sijiao L. Nanotechnology and biosensors. Biotechnol Adv. 2004;22(7):505-518. https://doi.org/10.1016/j.biotechadv.2004.03.004.

[4] Riu J, Maroto A, Rius FX. Nanosensors in environmental analysis. Talanta. 2006;69(2):288-301. https://doi.org/10.1016/j.talanta.2005.09.045.

[5] Scrimin P, Tecilla P. Model membranes: developments in functional micelles and vesicles. Curr Opin Chem Biol. 1999;3(6):730-735. https://doi.org/10.1016/S1367-5931(99)90031-5.

[6] Ding Y, Wang S, Li J, Chen L. Nanomaterial-based optical sensors for mercury ions. TrAC - Trends Anal Chem. 2016;82:175-190. https://doi.org/10.1016/j.trac.2016.05.015.

[7] Burguera JL, Burguera MJT. Analytical applications of organized assemblies for on-line spectrometric determinations: present and future. Talanta. 2004;64(5):1099-1108. https://doi.org/10.1016/j.talanta.2004.02.046.

[8] Kalinina M, Golubev N, Raitman O, Selector S, Arslanov V. A novel ultra-sensing composed Langmuir–Blodgett membrane for selective calcium determination in aqueous solutions. Sens Actuators B Chem. 2006;114(1):19-27. https://doi.org/10.1016/j.snb.2005.04.021.

[9] Ermakova EV, Koroleva EO, Shokurov AV, Arslanov VV, Bessmertnykh-Lemeune A. Ultra-thin film sensors based on porphyrin-5-ylphosphonate diesters for selective and sensitive dual-channel optical detection of mercury(II) ions. Dyes Pigm. 2021;186:108967. https://doi.org/10.1016/j.dyepig.2020.108967.

[10] Raza W, Kukkar D, Saulat H, Raza N, Azam M, Mehmood A, Kim KH. Metal-organic frameworks as an emerging tool for sensing various targets in aqueous and biological media. TrAC - Trends Anal Chem. 2019;120:115654. https://doi.org/10.1016/j.trac.2019.115654.

[11] Kubota R, Sasaki Y, Minamiki T, Minami T. Chemical sensing platforms based on organic thin-film transistors functionalized with artificial receptors. ACS Sens. 2019;4(10):2571-2587. https://doi.org/10.1021/acssensors.9b01114.

[12] Oliveira Jr ON, Caseli L, Ariga K. The past and the future of Langmuir and Langmuir–Blodgett films. Chem Rev. 2022;122(6):6459–6513. https://doi.org/10.1021/acs.chemrev.1c00754.

[13] Liu B, Zhuang J, Wei G. Recent advances in the design of colorimetric sensors for environmental monitoring. Environ Sci: Nano 2020;7(8):2195-2213. https://doi.org/10.1039/D0EN00449A.

[14] Mako TL, Racicot JM, Levine M. Supramolecular luminescent sensors. Chem Rev. 2019;119(1):322-477. https://doi.org/10.1021/acs.chemrev.8b00260.

[15] Krämer J, Kang R, Grimm LM, De Cola L, Picchetti P, Biedermann F. Molecular Probes, Chemosensors, and Nanosensors for Optical Detection of Biorelevant Molecules and Ions in Aqueous Media and Biofluids. Chem Rev. 2022;122(3):3459–3636. https://doi.org/10.1021/acs.chemrev.1c00746.

[16] Magri DC, Brown GJ, McClean GD, de Silva AP. Communicating chemical congregation: a molecular AND logic gate with three chemical inputs as a "lab-on-a-molecule" prototype. J Am Chem Soc. 2006;128(15):4950-4951. https://doi.org/10.1021/ja058295+.

[17] Magri DC, Fava MC, Mallia CJ. A sodium-enabled 'Pourbaix sensor': a three-input AND logic gate as a 'lab-on-a-molecule'for monitoring Na^+, pH and pE. Chem Commun. 2014;50(8):1009-1011. https://doi.org/10.1039/C3CC48075E.

[18] Chen K, Shu Q, Schmittel M. Design strategies for lab-on-a-molecule probes and orthogonal sensing. Chem Soc Rev. 2015;44(1):136-160. https://doi.org/10.1039/C4CS00263F.

[19] Ermakova E, Raitman O, Shokurov A, Kalinina M, Selector S, Tsivadze A, Arslanov V, Meyer M, Bessmertnykh-Lemeune A, Guilard R. A metal-responsive interdigitated bilayer for selective quantification of mercury(II) traces by surface plasmon resonance. Analyst. 2016;141(6):1912-1917. https://doi.org/10.1039/C5AN02523K.

[20] Arslanov V, Ermakova E, Michalak J, Bessmertnykh-Lemeune A, Meyer M, Raitman O, Vysotskij V, Guilard R, Tsivadze A. Design and evaluation of sensory systems based on

amphiphilic anthraquinones molecular receptors. Colloids Surf A: Physicochem Eng Asp. 2015;483:193-203. https://doi.org/10.1016/j.colsurfa.2015.05.016.

[21] Kaur B, Kaur N, Kumar S. Colorimetric metal ion sensors–A comprehensive review of the years 2011–2016. Coord Chem Rev. 2018;358:13-69. https://doi.org/10.1016/j.ccr.2017.12.002.

[22] Anzenbacher Jr P, Mosca LM. Optical Probes and Sensors. Supramolecular Chemistry in Water. 2019:449-499. https://doi.org/10.1002/9783527814923.ch12.

[23] Zhang Q, Huang Y, Wang Y, Li S, Jiang Y. Modular fabrication of fluorescent sensors via hydrogen-bonding self-assembly. Dyes Pigm. 2019;169:111-117. https://doi.org/10.1016/j.dyepig.2019.05.011.

[24] El-Safty SA, Shenashen MA. Mercury-ion optical sensors. TrAC - Trends Anal Chem. 2012;38:98-115. https://doi.org/10.1016/j.trac.2012.05.002.

[25] Daware K, Shinde R, Kalubarme RS, Kasture M, Pandey A, Terashima C, Gosavi SW. Development of optical sensing probe for Hg(II) ions detection in ground water using Au, Hexanedithiol and Rhodamine B nanocomposite system. Sens Actuators B Chem. 2018;265:547-55. https://doi.org/10.1016/j.snb.2018.03.095.

[26] Kou D, Ma W, Zhang S. Functionalized Mesoporous Photonic Crystal Film for Ultrasensitive Visual Detection and Effective Removal of Mercury(II) Ions in Water. Adv Funct Mater. 2021;31(9):2007032. https://doi.org/10.1002/adfm.202007032.

[27] Shi Y, Liu Z, Liu R, Wu R, Zhang J. DNA-Encoded MXene-Pt Nanozyme for Enhanced Colorimetric Sensing of Mercury Ions. Chem Eng J. 2022;442(1):136072. https://doi.org/10.1016/j.cej.2022.136072.

[28] Ermakova E, Michalak J, Meyer M, Arslanov V, Tsivadze A, Guilard R, Bessmertnykh-Lemeune A. Colorimetric Hg^{2+} sensing in water: From molecules toward low-cost solid devices. Org Lett. 2013;15(3):662-665. https://doi.org/10.1021/ol303499v.

[29] Langdon-Jones EE, Pope SJ. The coordination chemistry of substituted anthraquinones: Developments and applications. Coord Chem Rev. 2014;269:32-53. https://doi.org/10.1016/j.ccr.2014.02.003.

[30] Ghosh A, Jose DA, Kaushik R. Anthraquinones as versatile colorimetric reagent for anions. Sens Actuators B Chem. 2016;229:545-560. https://doi.org/10.1016/j.snb.2016.01.140.

[31] Busschaert N, Caltagirone C, Van Rossom W, Gale PA. Applications of supramolecular anion recognition. Chem Rev. 2015;115(15):8038-8155. https://doi.org/10.1021/acs.chemrev.5b00099.

[32] Kaur N, Kumar S. Colorimetric recognition of Cu (II) by (2-dimethylaminoethyl) amino appended anthracene-9,10-diones in aqueous solutions: deprotonation of aryl amine NH responsible for colour changes. Dalton Trans. 2006(31):3766-3771. https://doi.org/10.1039/B601558A.

[33] Kumar S, Kaur N. Nature of 1-(2-aminoethylamino)-anthracene-9,10-diones-Cu (II) interactions responsible for striking colour changes. Supramol Chem. 2006;18(2):137-140. https://doi.org/10.1080/10610270600564686.

[34] Anderson DJ. Determination of the lower limit of detection. Clin Chem. 1989;35(10):2152-2153. https://doi.org/10.1093/clinchem/35.10.2152.

[35] Huang T, Toraya H, Blanton T, Wu Y. X-ray powder diffraction analysis of silver behenate, a possible low-angle diffraction standard. J Appl Crystallogr. 1993;26(2):180-184. https://doi.org/10.1107/S0021889892009762.

[36] Beletskaya IP, Bessmertnykh AG, Averin AD, Denat F, Guilard R. Palladium-Catalysed Amination of 1,8- and 1,5-Dichloroanthracenes and 1,8- and 1,5-Dichloroanthraquinones. Eur J Org Chem. 2005;2005(2):281-305. https://doi.org/10.1002/ejoc.200400455.

[37] Ranyuk E, Uglov A, Meyer M, Bessmertnykh-Lemeune A, Denat F, Averin A, Beletskaya I, Guilard R. Rational design of aminoanthraquinones for colorimetric detection of heavy metal

ions in aqueous solution. Dalton Trans. 2011;40(40):10491-10502. https://doi.org/10.1039/C1DT10677E.

[38] Fukuda K, Nakahara H, Kato T. Monolayers and multilayers of anthraquinone derivatives containing long alkyl chains. J Colloid Interface Sci. 1976;54(3):430-438. https://doi.org/10.1016/0021-9797(76)90323-4.

[39] Ishikawa Y, Kunitake T, Matsuda T, Otsuka T, Shinkai S. Formation of calixarene monolayers which selectively respond to metal ions. Chem Commun. 1989(11):736-738. https://doi.org/10.1039/C39890000736.

[40] US EPA GWaDW, National Primary Drinking Water Regulations (NPDWR). https://www.epa.gov/ground-water-and-drinking-water/national-primary-drinking-water-regulations#Inorganic (accessed 02 May 2022).

[41] Maâtouk F, Maâtouk M, Bekir K, Barhoumi H, Maaref A, Ben Mansour H. An electrochemical DNA biosensor for trace amounts of mercury ion quantification. J Water Health. 2016;14(5):808-815. https://doi.org/10.2166/wh.2016.293.